24th INTERNATIONAL CONGRESS ON SOUND AND VIBRATION
23–27 July 2017, London

ACOUSTIC DESIGN OF A BEST-IN-CLASS DRILL RIG CABIN

Jukka Tanttari and Lasse Lamula

VTT Technical Research Centre of Finland Ltd, Tampere, Finland
email: jukka.tanttari@vtt.fi

Drill rigs used for percussive rock drilling are sources of intense high-frequency noise. A drill rig manufacturer targeted the in-cabin A-weighted noise level at the operator's position during drilling to be less than 75 dB. The target sets very strict demands on the noise reduction capability of a cabin. As is well known, considerable modifications to a final product are very difficult. Therefore, the cabin acoustic design process, described in this paper, was started eighteen months before the manufactured cabin was available for assessment. Thanks to the early, proactive start, the result is a cabin with an excellent acoustic performance and the target was successfully met. The most critical cabin component group is glazing, which covers some 40 % of the outer surface of the cabin. Much effort was put on simulation-based acoustic design, optimization and selection of thick, multi-layer laminated glasses. Another critical factor emphasized is control of leakage, especially avoidance of imperceptible leaks in door seals, plate junctions etc. Due to the harsh working environment, the possibility to use porous materials for enhanced absorption is very limited. Numerical simulations using SEA and experiments conducted in various phases of the process are described. Experimental results of the final product are compared to early predictions and updated simulations. Uncertainties arising from incomplete data available in the early design stages, rig operating environment as well as from the methods themselves are discussed. Keywords: low noise design, cabin acoustics, SEA, noise reduction

1. Introduction

Surface drill rigs (Fig. 1) are used to drill holes into rock. Longitudinal stress waves, generated to a drill rod by a percussion drill, are lead to the rock-breaking bit. Intense broadband drilling noise, dominated by radiation from flexural waves in the drill rod [1] is generated. The A-weighted maximum of drilling noise occurs at the frequency range 500…4000 Hz. Cabins of modern drill rigs are designed for the highest class of comfort. Demands for the noise reduction capability of the cabin are strict.

Figure 1: A typical drill rig.

2. Timeline and goals

The goal was to create a best-in-class, low-noise cabin with A-weighted SPL 75 dB or less during drilling. This means that the Noise Reduction (difference between exterior and interior A-weighted levels) must be 35 dB or more.

The acoustic subproject started immediately after the cabin initial design was available. The timeline is depicted in Fig. 2.

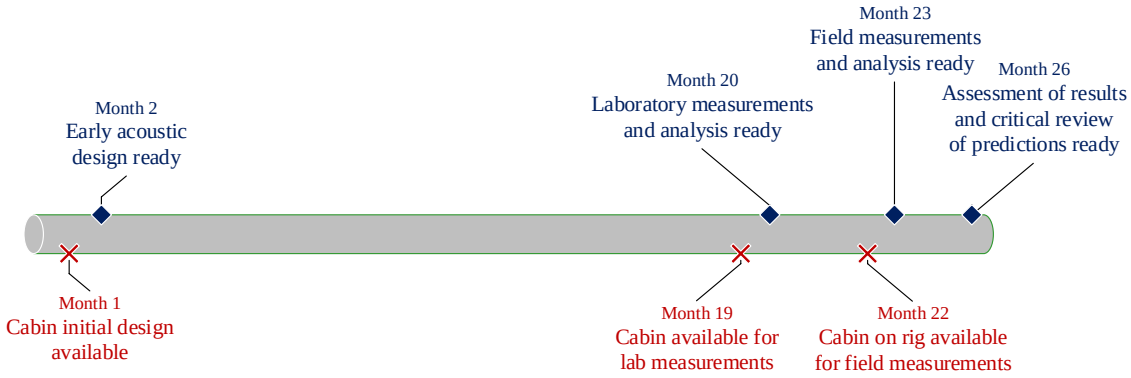

Figure 2: Timeline of the project seen from the acoustic design point of view.

As is well known, considerable modifications to a final product are very difficult. A major effort was therefore put on modelling-based early acoustic design of the cabin ("early phase"). After an intense phase of work in the company, the first physical copy of the cabin was available for experiments 18 months later. Some refinements were expected to be necessary in the prototype phase.

3. Acoustic design in the early phase

3.1 Starting points

The overall geometry of the cabin, mechanical strength (i.e., the steel structure) and visibility from the cabin were already given in the initial design. Many details were expected to change as the process proceeded.

The cabin steel panels are 3 or 4 mm thick and they cover roughly 60 % of the surface. It was assumed, that a damping treatment could be applied on most of the steel panels, if needed. The interior trim was assumed to consist of a 30…40 mm air gap and a few millimetres thick, durable plastic cladding. The assumed floor coating was a two-layer (soft foam + heavy rubber) mat.

The operating environment of a drill rig is harsh and dusty. The possibility to tune interior acoustics using porous fibrous or foam materials is very limited. The expected sound absorption of the cabin is modest. The main sources of absorption are the bench and the operator.

The glazing covers 40 % of the exterior surface. Acoustic excitation due to drilling is highest at the glazing, especially at the windscreen, roof window and the large window on the right side of the cabin. Apart from some surface mass and thickness restrictions, the properties of the glazing were not specified in the initial cabin design. They were in the focus in the early phase of the acoustic design.

Avoidance of leaks by thorough design and accurate manufacturing is especially important and was emphasized in the design of the cabin. There was an opening defined for ventilation, but no information on the associated equipment was available in the early phase.

A vital factor in SPL predictions are exterior acoustic loads. Load data from existing rigs measured in the past were used. Based on previous experience, contributions of direct structural excitation of the cabin, as well as engine noise, were assumed to be insignificant.

The cabin represents an archetypal complex system with uncertain details. It is well known that SEA, utilizing average properties of a population of similar structures with differences in details, is an ideal tool for this kind of situation [2], especially for the case of high-frequency random loads.

SEA has been successfully used for cabins in the past [3, 4]. The SEA module within VA One software [5] was used in the SEA-models and simulations described below.

3.2 Early phase SEA models

The SEA model is depicted in Fig. 3. The model consists of one acoustic subsystem, 91 structural subsystems and 400 junctions. Altogether, 18 different model variants were built and analysed in the early phase. Most of the variants were used for the assessment of different glazing alternatives. Some models included also different combinations of damping treatments and floor mats. Separate component models were used for a thorough analysis on acoustic properties of multi-layered laminated glass. With the initial acoustic loads the scatter of predicted A-weighted cabin level was 71…79 dB depending on model variant.

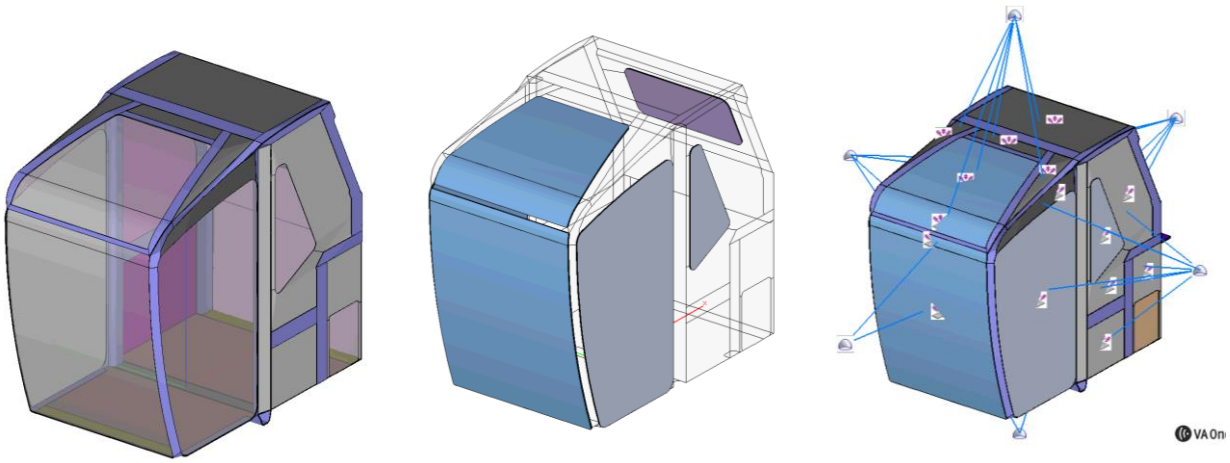

Figure 3: SEA-model of the cabin. Left: steel structure, centre: glazing, right: whole cabin with exterior acoustic loads and field connections.

3.3 Vibro-acoustic analysis and tailoring of glazing properties

The first calculations showed clearly, that the insulation of the steel structure with the assumed trim would be sufficient, but sound insulation of glazing is critical for reaching the target. Much effort was therefore put on the vibro-acoustic design of the glazing.

Relatively thick glass, up to approximately 13 mm, was defined for the key windows (windshield, roof, window on right side of the cabin). Somewhat thinner glass was defined for the door and the rear window.

The combination of high-frequency acoustic excitation, high thickness and the mechanical properties of glass are problematic from the sound insulation point of view. A monolithic 13 mm thick glass has a deep coincidence dip in the transmission loss (*TL)* around 1 kHz. The poor acoustic performance is (*i*) due to ratio of flexural rigidity and surface mass causing acoustically fast waves and hence efficient coupling with air and (*ii*) low inherent material damping loss factor of glass.

Laminated glass (Fig. 4) consists of glass layers bonded together using visco-elastic interlayers. The interlayers have a safety function for the case the window is broken.

The layering (the thickness and material of each layer) has a strong effect on the vibro-acoustic performance as well. This is based on strong shear deformation in the interlayers. There are also special “acoustic” interlayers available. They have much lower shear modulus and much higher damping loss factor compared to the standard PVB-interlayers. When properly designed, acoustical properties of a thick laminated glass can be enhanced greatly using a proper combination of glass and interlayers [6, 7].

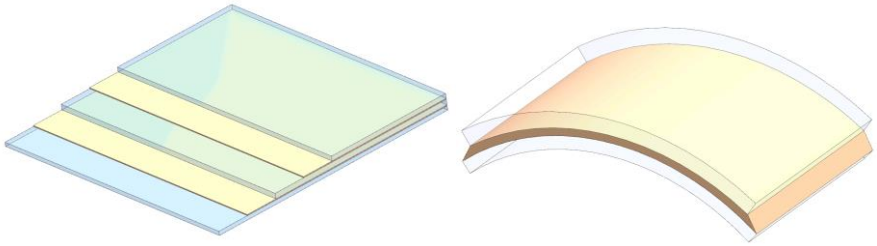

Figure 4: Laminated glass and schematic shear deformation of a visco-elastic interlayer in flexure.

It is not practical to search for good vibro-acoustic properties for a thick, multi-layer laminated glass by trial and error. The General Laminate theory [8], combining a spectral element model of the laminate cross-section and the SEA-model were used with optimization tools available in VA One. The number of models solved during an optimization run was from a few hundred to more than ten thousand, depending on the laminate properties. In practice, an alternative not too far from the optimal solution (i.e., thicknesses of individual layers) were then chosen.

Key vibro-acoustic properties of three variants of a 12.28 mm thick glass are shown in Fig. 5. The critical frequency (i.e., coincidence dip) of a multilayer glass can be two octaves higher than that of a monolithic glass and its *TL* at important frequencies up to 20 dB higher. Using interlayers, the *TL* can be increased over practically the whole frequency range as the transmission mechanism changes from damping-controlled (resonant) to mass-controlled. The standard 3-layer glass is, due to higher damping, better than the monolithic glass, but clearly worse than the multilayer solution.

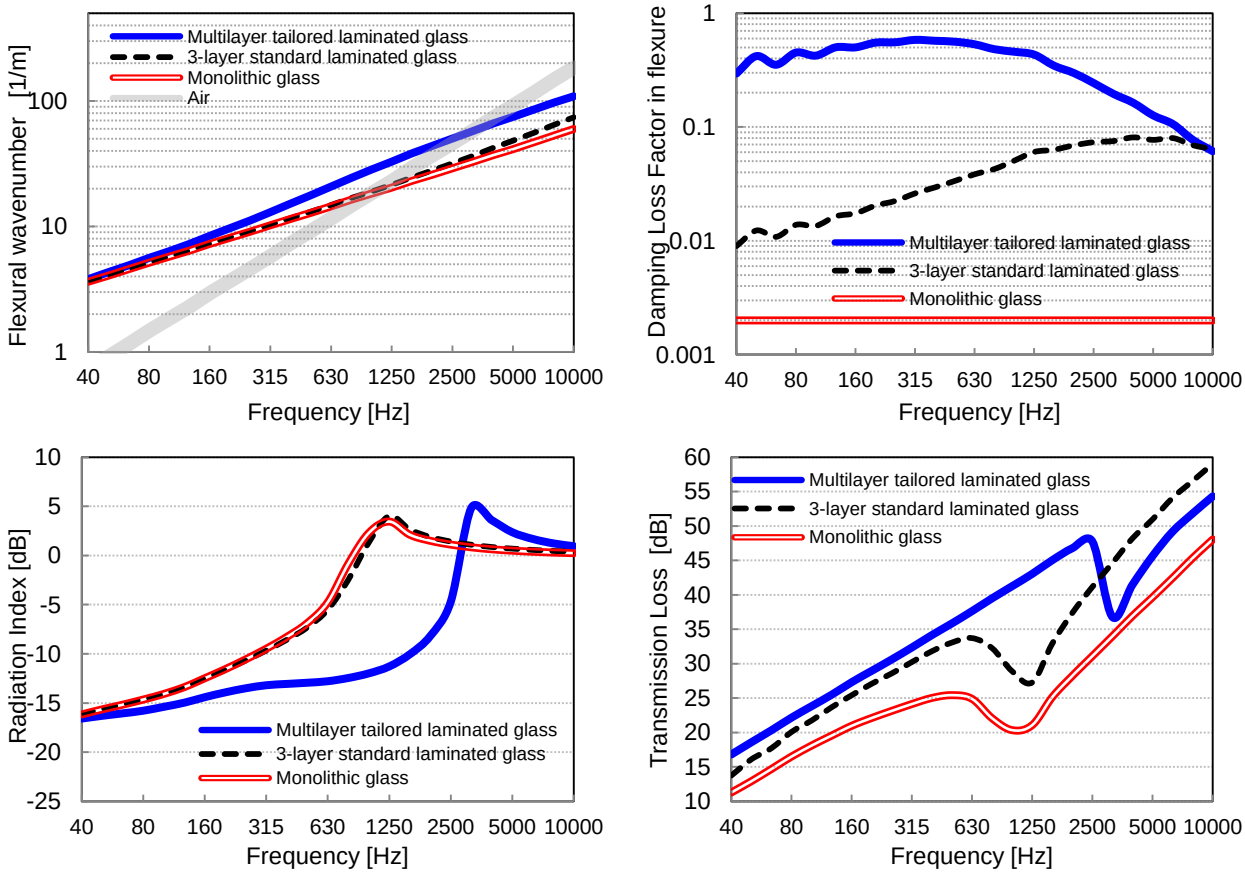

Figure 5: Vibro-acoustic properties of 12.28 mm thick glass of surface area 1.36 m^2. Top left: wave-number, top right: damping loss factor, bottom left: radiation index, bottom right: *TL*.

The mechanical properties needed in calculations were determined using tests of laminated glass beams. The interlayers were assumed to be linearly visco-elastic with frequency-dependent shear modulus and damping loss factor. The properties are known to be strongly temperature-dependent. The calculations were done for 20°C.

4. Results

4.1 Experiments of a separate cabin

The noise reduction capability of the first available cabin was determined in the laboratory with the so called CAB-analysis [9]. The cabin was mounted on a stand in a semi-anechoic room and the floor beneath the cabin was covered with absorption material. An omnidirectional loudspeaker was placed inside the cabin. The surface of the cabin was divided into subareas and sound pressure levels were measured both inside and outside of every surface. The division into sub-areas followed structural details of the cabin.

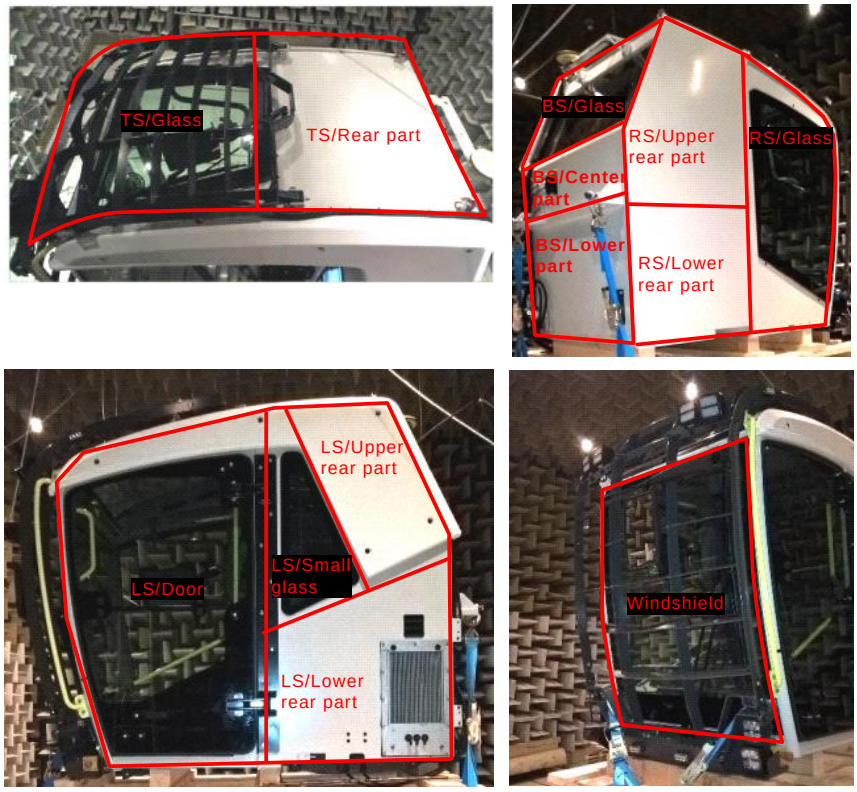

Figure 6: Sub-areas used in the CAB-analysis.

The sound pressure levels transmitted into the cabin were calculated based on the determined noise reductions using exterior excitation noise spectra measured in situ. At this stage the actual exterior noise data was not available since since the cabin had not been used on an actual rig. Therefore the data from a previously studied drill rig was utilized.

The above analysis gives information about the main sound transmission paths and an estimate of the predicted noise level in the cabin. Noise reduction modifications can be introduced and their effect on the sound pressure levels inside the cabin can be assessed.

In addition to the CAB-analysis, the sound field on the exterior surfaces of the cabin due to the interior loudspeaker excitation was visualized with the Scan&Paint method [10]. In the Scan&Paint method the surface is scanned with a special probe measuring the sound pressure and sound particle velocity. At the same time a video camera is aimed at the surface to capture the scanning. The recorded video and audio data are automatically synchronized by the software. A high resolution sound color map is produced as a result.

The analysis gives an estimate of the sound pressure level inside the cabin due to different subareas (Fig. 7). The figure shows also shares of the subareas as percentage. The noise reduction of the cabin appears to be evenly distributed except that the left side is responsible for 53.5 % of the sound transmission. The worst subarea is the lower rear part of the left side (36.8 %), which is almost totally due to the air conditioning grille (Fig. 8). Another sound leakage is in the rear lower corner of

the door. The reason for the leakage was a small area, where the door sealing was poorly compressed.

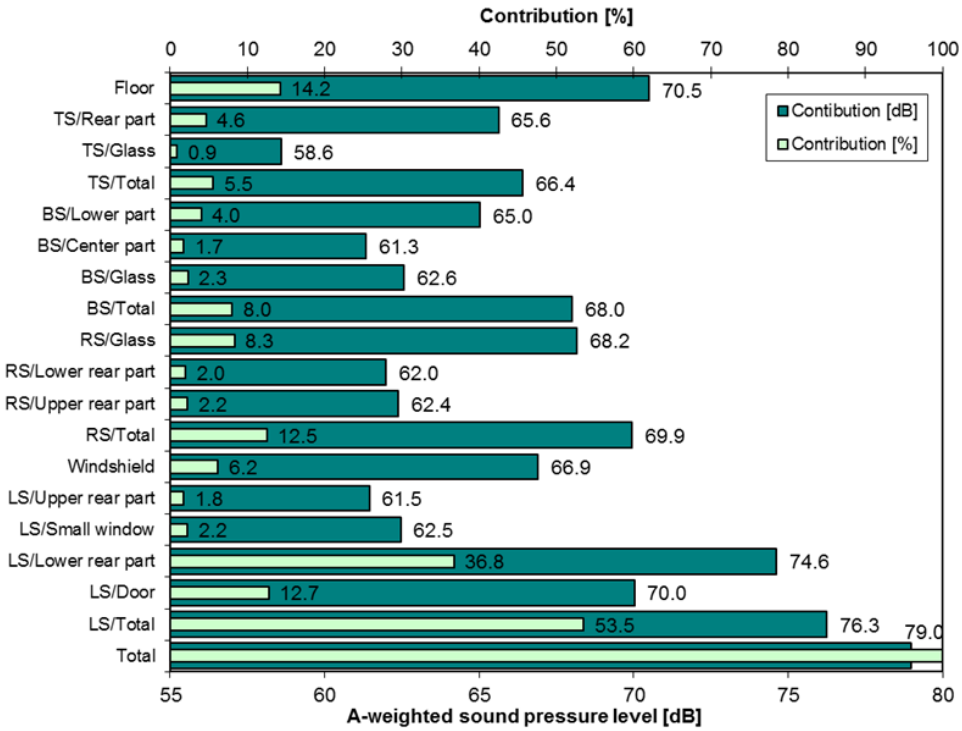

Figure 7: The order of importance of the subareas as a noise transmission path.

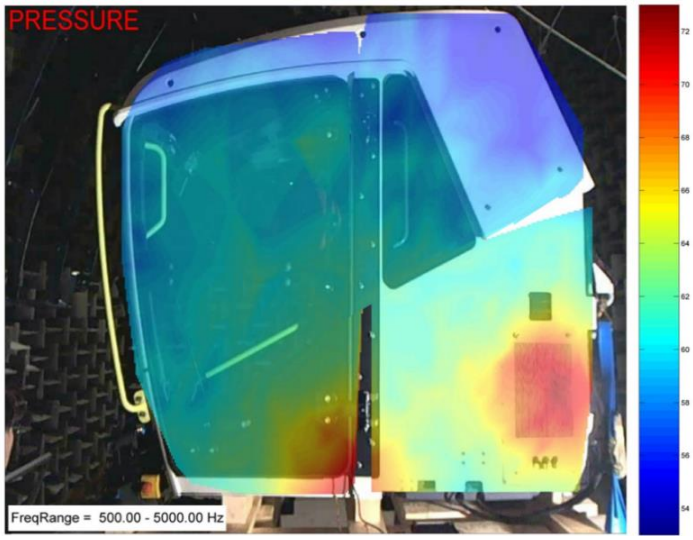

Figure 8: Sound pressure level map pinpointing the problematic air conditioning grille and leaking corner of the cabin door.

4.2 Final measurements in operating conditions

When the cabin was mounted on an actual drill rig, it was possible to re-analyse the transfer paths with the actual measured exterior excitation data (Fig. 9). Now the left side is responsible for 48.7 % of the sound transmission (earlier prediction 53.5 %). The most critical subareas are the door (15.5 %) and left side lower rear part (29.6 %) where the air conditioning grille is located. Thus the air conditioning grille is not as critical as estimated earlier, but still it is the weakest point of the cabin and an apparent choice for actions if further improvement is considered. The total contribution of all glass surfaces is 41 %

The calculated noise spectrum in the cabin with the measured excitation of the new rig is given in Fig. 10. The estimated A-weighted total level with the actual excitation is only 4 dB higher than what was measured. The reasons for the differences below 500 Hz are discussed in chapter 5. The high level estimates at 6.3-10 kHz are caused by measurement equipment noise because in the CAB analysis with loudspeaker excitation the levels outside the cabin are very low at those frequencies.

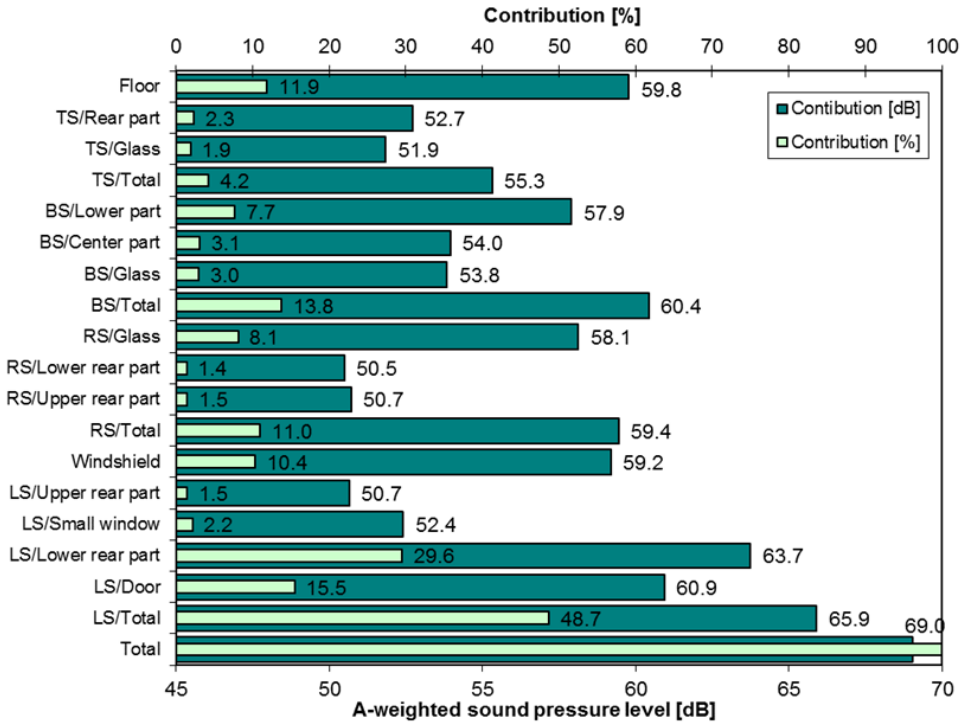

Figure 9: Re-analysis of the transfer paths with the actual measured exterior excitations.

4.3 Results of updated SEA-model

In the last phase of the project, the SEA model including the loads was updated to be consistent with the measured cabin. The A-weighted sound pressure calculated using the updated model is 66.5 dB compared to the measured value of 65.0 dB. The predicted and measured A-weighted spectra are in Fig 10. The main updates are listed below.

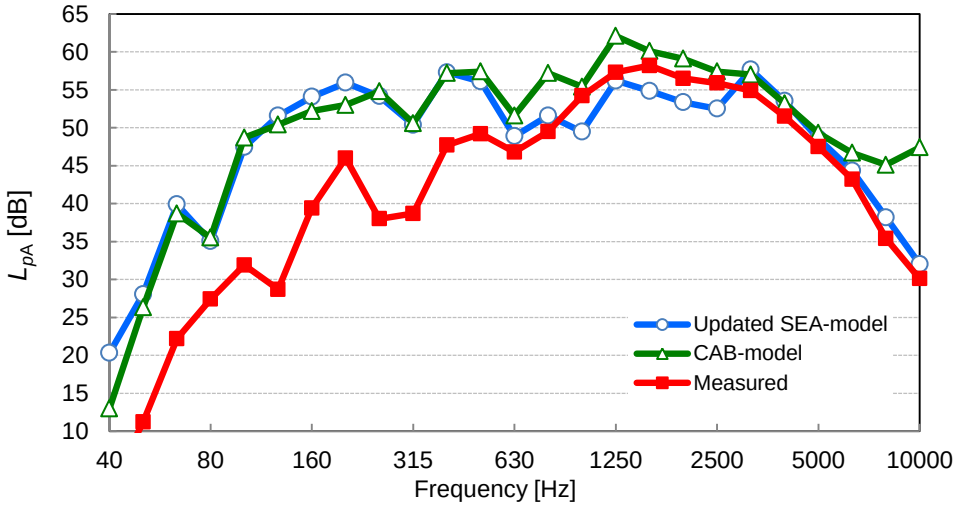

Figure 10: Predicted and measured A-weighted spectra.

- Absorption coefficient was increased: there is some porous material on the ceiling.
- A porous lagging (mainly for thermal isolation) was added on inner surfaces of wall panels.
- Amount of damping treatment on steel panels was reduced.

- Sound transmission property of the ventilation box was added to the updated model.
- Properties of the glazing were updated.

The contribution of glazing calculated using the updated SEA model, 34.5 %, is in good agreement with the experimental CAB-result 41.0 %. The most significant difference between the SEA and experimental result is due to the leak at door seal. The leak was not defined in the SEA-model.

5. Discussion on prediction uncertainties

The most notable difference between the predicted and measured cabin sound pressure levels is the low frequency over-prediction (Fig. 10). It is common to CAB- and SEA-methods; the spectral shapes are very similar. The root cause is that at low frequencies (below the cabin Schroeder frequency at 500 Hz), sound pressure is systematically lower in the interior of the cabin (at the location of operator's head) compared to pressure near the surfaces. Both the CAB- and SEA-methods average over the inner surfaces (CAB) or the whole volume (SEA). Thus they do not take this systematic effect into account. The phenomenon was analysed and confirmed using a BEM-model of the interior.

Another major source of uncertainty is the operational loads arising from uncontrollable variation of operating and environmental conditions. The mutual distance between drill rod and the cabin as well as properties of the ground may cause a deviation of roughly several decibels.

6. Concluding remarks

The goal of the project was fulfilled. A best-in-class, low-noise cabin with A-weighted SPL considerable lower than 75 dB during drilling was created. The key to the success was the early, proactive start of the acoustic design followed by thorough experimental analyses.

7. Acknowledgement

The authors wish to thank Sandvik Mining and Rock Technology for the financial support and opportunity to publish the results in this paper.

REFERENCES

1 Tanttari, J. On the drill rod noise in percussive rock drilling. *Nordic Acoustical Meeting NAM 96*. Helsinki 12-14 June 1996. p. 121-128.

2 Shorter, P. Modeling noise and vibration transmission in complex systems. In: A.K. Belyaev, R.S. Langley (eds.), *IUTAM Symposium on the Vibration Analysis of Structures with Uncertainties*, IUTAM Book series 27, Springer 2011. p. 141 – 156.

3 Nousiainen E. and Tanttari J. Acoustic characterization of electric connectors and use of the data in tractor cabin SEA-models. *Forum Acusticum 2002*. Sevilla, Spain, 16.-20.9.2002.

4 Pietila, G. Noise and Sound Quality Optimization of Agricultural Machine Cab. *SAE Commercial Vechile Conference*, May 2010. SAE 10CV_0211. 14 p.

5 VA One software, versions 2014.5, 2015, 2016. ESI Group, 2014-2016.

6 Lu, J. Passenger Vehicle Interior Noise Reduction by Laminated Side Glass. *inter-noise 2002*, Dearborn, MI, USA, August 19-21, 2002. 8 p.

7 Bouayed, K. and Hamdi, M. Dynamic behavior of laminated windscreen. *J. Acoust. Soc. Am*. **132** (2), 757-766, (2012).

8 Shorter, P.J. Wave propagation and damping in linear viscoelastic laminates. *J. Acoust. Soc. Am*. **115 (**5), 1917–1925, (2004).

9 Tanttari, J. and Saarinen, K. Noise control of vehicle cabins. *Proceedings of Internoise 93*, Leuven Belgium, 24-26 August, (1993).

10 Comesaña, D.,F., Steltenpool, S., Pousa, G.,C., de Bree and H., Holland, K., R. Scan and Paint: Theory and Practice of a Sound Field Visualization Method, *ISRN Mechanical Engineering*, vol. 2013, Article ID 241958, 11 pages, 2013. doi:10.1155/2013/241958